Calcium-dependent molecular fMRI using a magnetic nanosensor

Satoshi Okada†, Benjamin B. Bartelle†, Nan Li, Vincent Breton-Provencher, Jiyoung Lee, Elisenda Rodriguez, James Melican, Mriganka Sur & Alan Jasanoff*

† equal contribution
* correspondence to AJ (*jasanoff@mit.edu*)

Supplementary Table S1. DNA sequence of C2AB^{Ca-}. Aspartate and glutamate residues involved in Ca^{2+} binding were mutated to alanine. Corresponding sequence changes are indicated by red and blue respectively. Start and stop codons are underlined.

ATGGGGGGTTCTCATCATCATCATCATCATGGTATGGCTAGCATGACTGGTGGACAGCAAATGGGTCGGGA
TCTGTACGACGATGACGATAAGGATCGATGGGGATCCGAGCTCGAGATCTTCAAAGATGGAAAGGGTAAGA
AGGGTGTCGACATGAAGTCGGTACAGTTGTTGGGATCGGCGTACAAGGAGAAACCTGATATGGAGGAACTC
ACCGAAAATGCCGAGGAGGGTGACGAGGAGGACAAGCAGAGCGAGCAGAAGCTGGGGCGCCTCAACTTCAA
GCTGGAATACGATTTCAACTCCAACAGTTTGGCCGTGACGGTGATCCAAGCCGAGGAGCTTCCCGCCCTGG
CTATGGGCGGTACCTCGGCTCCCTATGTCAAGGTGTACTTGCTGCCCGACAAGAAGAAGAAGTTCGAGACC
AAGGTGCACCGCAAGACACTGAGTCCGGTCTTCAACGAGACGTTCACCTTTAAGAGTTTGCCCTACGCCGA
TGCCATGAACAAGACGCTCGTGTTTGCCATTTTCGCCTTCGCTCGCTTCTCGAAGCACGCCCAGATCGGCG
AGGTGAAGGTGCCGCTGTGCACCATCGATCTGGCGCAGACAATCGAGGAGTGGCGCGACCTGGTCAGCGTT
GAAGGAGAGGGCGGACAGGAAAAGCTGGGAGATATCTGCTTCTCGCTGCGCTACGTGCCGACCGCCGGAAA
GCTAACCGTCGTCATCCTGGAGGCCAAGAACTTGAAGAAGATGGCCGTGGGCGGACTGTCTGCCCCATATG
TGAAAGTTGCAATCATGCAAAATGGCAAACGTTTGAAAAAGAAGAAGACAAGTGTCAAAAAATGCACCCTC
AACCCTTACTATAATGAGTCGTTCTCATTTGAAGTACCATTTGAACAAATGCAAAAAATCTGTCTCGTTGT
GACCGTCGTGGCCTACGCCCGTATTGGCACCTCCGCACCCATCGGCCGCTGCATACTTGGCTGCATGGGCA
CCGGAACCGAGCTGCGTCACTGGTCGGACATGTTGGCCTCGCCCCGCCGGCCCATCGCCCAGTGGCACACC
CTCAAGGATCCCGAGGAGACCGACGAGATCCTGAAGAACATGAAGTAA

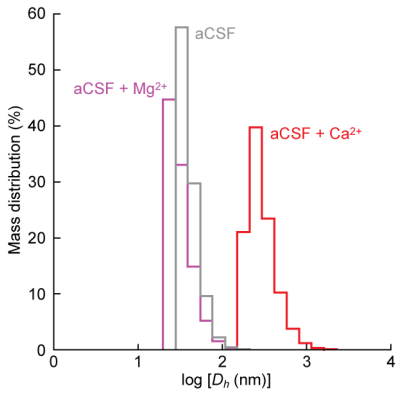

Supplementary Figure S1. Specificity of MaCaReNas for Ca^{2+} vs. Mg^{2+}. Mass distribution of the hydrodynamic diameter of MaCaReNa measured by DLS in Ca^{2+}-free aCSF (gray), aCSF containing 1 mM Ca^{2+} (red), or aCSF with calcium substituted by 1 mM Mg^{2+} (purple). Nanoparticle [Fe] = 100 μM and [C2AB] = 2.5 μM.

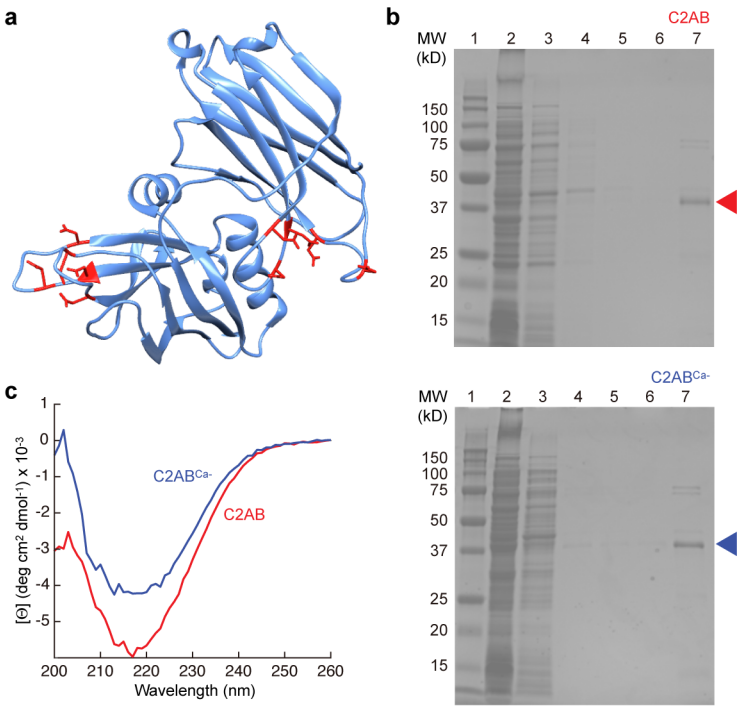

Supplementary Figure S2. Design and characterization of C2AB^{Ca-}. (a) Structure of synaptotagmin 1 C2AB (human variant shown[35]) illustrating sites of alanine substitution for creation of the C2AB^{Ca-} mutant. **(b)** Coomassie brilliant blue-stained 12% SDS-PAGE following Ni-NTA affinity purification of 6XHis-tagged C2AB (top) and C2AB^{Ca-} (bottom). Lanes denote (1) protein standard, (2) Ni-NTA flowthrough fraction, (3-6) wash fractions, and (7) Ni-NTA elution fraction. Arrowheads denote bands corresponding to purified proteins. **(c)** Circular dichroism spectra of C2AB (red) and C2AB^{Ca-} (blue) in 10 mM potassium phosphate buffer (pH 7.4), indicating comparable secondary structure content of both molecules. Experiments were performed using a Model 202 circular dichroism spectrometer (Aviv Biomedical) operated at room temperature. Absorbance at 280 nm of the sample solution was adjusted to ~0.8 prior to measurement.

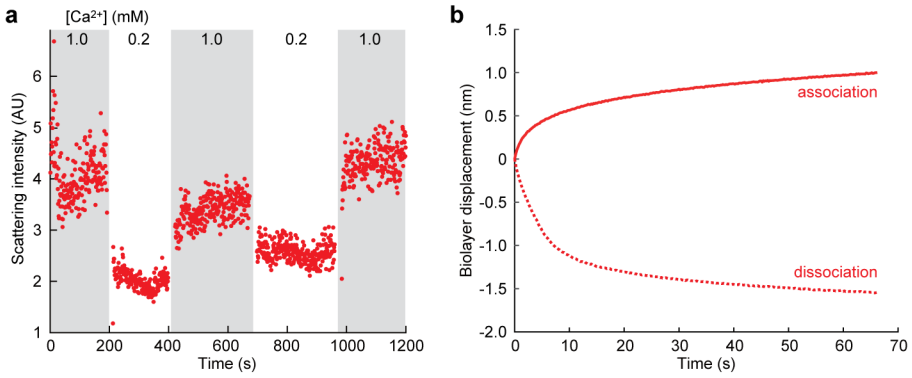

Supplementary Figure S3. Kinetics of MaCaReNa responses. (a) Time course of scattering intensity measured by DLS, illustrating reversible responses of MaCaReNas to alternating calcium concentrations. Measurements began in aCSF containing 1 mM Ca^{2+}. Addition of BAPTA or $CaCl_2$ produced subsequent switches between 0.2 mM and 1.0 free [Ca^{2+}], each with an approximately 20 s dead time for buffer addition and mixing. Nanoparticle [Fe] = 100 µM and [C2AB] = 2.5 µM. **(b)** Biolayer interferometry study of LCIO association (solid line) and disassociation (dashed line) from C2AB immobilized on a BLI probe tip.

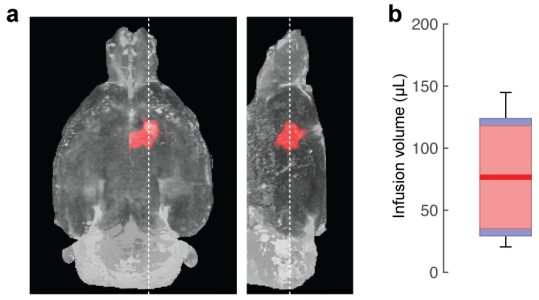

Supplementary Figure S4. Volume of nanoparticle infusion into rat brain. (a) Maximum intensity projection of an *ex vivo* rat brain at 100 µm resolution. Left, horizontal image; right, sagittal image (relative positions denoted by dotted lines). Colored region denotes a segmented hypointense volume around the area of *in vivo* intracranial injection of LCIOs. (**b**) Volumetric analysis of nanoparticle spread in four animals. Whiskers denote limits of variance, blue lines denote standard deviation, and red line denotes the mean volume.

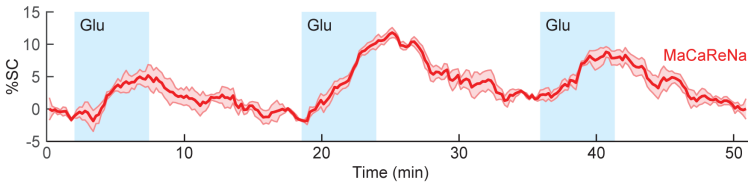

Supplementary Figure S5. Time course of MaCaReNa based signal changes. Average time course (red trace) of molecular fMRI signal during three consecutive glutamate stimuli (blue shading), showing reproducibility of MaCaReNa responses (n = 4). Shading denotes SEM.

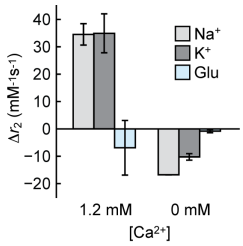

Supplementary Figure S6. Effects of chemical stimulants on MaCaReNa relaxivity *in vitro*. Reported Δr_2 values represent differences of MaCaReNa r_2 in aCSF supplemented with 100 mM Na^+, 100 mM K^+ and 1 mM glutamate compared with r_2 measured without the supplements (means ± SEM, $n = 3$). Values observed at 1.2 mM Ca^{2+} (similar to basal $[Ca^{2+}]_o$) and at 0 mM Ca^{2+} are shown.

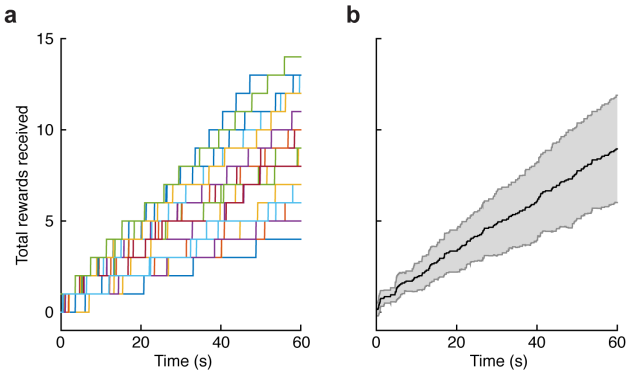

Supplementary Figure S7. MFB stimulation parameters used in MRI support operant behavior. (**a**) Time courses of self-stimulation measured from two rats tested in an operant box as described in the Methods section. Separate colors denote data from individual trails (20 total). **(b)** Average number of rewards as a function of time from the trials in panel (a). Shading denotes standard deviation over trials. Stimuli used in these experiments matched parameters used for fMRI experiments in Figure 4 (3 s trains of 200 Hz, 0.3 mA, 1 ms pulses). Spontaneously self-administered stimulation rates up to 14 trains per 60 s trial approximate the rate of six trains per 24 s stimulation block used for the experiments of Figure 4.